Constraints on the centroid moment tensors of the 2010 Maule and 2011 Tohoku earthquakes from radial modes

E. Zábranová,[1] C. Matyska,[1] L. Hanyk,[1] and V. Pálinkáš[2]

Received 21 June 2012; revised 14 August 2012; accepted 14 August 2012; published 21 September 2012.

[1] Surface acceleration caused by the radial modes depends only on the M_{rr} component of the centroid moment tensor and on its depth assuming the isotropic component to be negligible. The ${}_0S_0$-mode amplitude enables one to obtain a relatively narrow interval of M_{rr} values, whereas ${}_1S_0$-mode amplitude is more sensitive to centroid depth. We have used these facts to analyze the 2010 Maule (Chile) M_w = 8.8 and 2011 Tohoku (Japan) M_w = 9.1 earthquakes using PREM. Superconducting gravimeter data available within the framework of the Global Geodynamic Project reveal that the M_{rr} components of these earthquakes should be in the interval 0.95–1.15 × 10^{22} Nm (Maule) and 1.50–1.75 × 10^{22} Nm (Tohoku), respectively. Re-evaluation of the modal quality factors Q is needed to obtain constraints on M_{rr} self-consistently. The joint analysis of gravity data from both events yields Q = 5500 ± 140 for the ${}_0S_0$ mode and Q = 2000 ± 80 for the ${}_1S_0$ mode. We were not able to determine the quality factor of the ${}_2S_0$ mode with an accuracy sufficient to allow meaningful constraints (Q = 1120 ± 270). **Citation:** Zábranová, E., C. Matyska, L. Hanyk, and V. Pálinkáš (2012), Constraints on the centroid moment tensors of the 2010 Maule and 2011 Tohoku earthquakes from radial modes, *Geophys. Res. Lett.*, *39*, L18302, doi:10.1029/2012GL052850.

1. Introduction

[2] The source mechanism of the 2011 Tohoku M_w = 9.1 earthquake was first shown by rapid solutions published a few minutes and hours after the event (*Nettles et al.* [2011] (abbreviated as PS1 in Figure 3), *Polet and Thio* [2011] (PS2), *Duputel et al.* [2011] (PS3), *Hayes et al.* [2011], and *Shao et al.* [2011]) and then studied in detail by means of various seismic data sets: teleseismic and regional body and surface waves [*Koper et al.*, 2011; *Yokota et al.*, 2011; *Zhang et al.*, 2011] and strong motions [*Honda et al.*, 2011; *Kurahashi and Irikura*, 2011; *Suzuki et al.*, 2011; *Yoshida et al.*, 2011]. Similarly, there are rapid solutions available for the 2010 Maule M_w = 8.8 earthquake (G. Ekström and M. Nettles, http://earthquake.usgs.gov/earthquakes/eqinthenews/2010/us2010tfan/neic_tfan_cmt.php, 2010 (abbreviated as PS1 in Figure 2) and USGS, http://earthquake.usgs.gov/earthquakes/eqinthenews/2010/us2010tfan/neic_tfan_cmt.php, 2010 (PS2) and http://earthquake.usgs.gov/earthquakes/eqinthenews/2010/us2010tfan/neic_tfan_wmt.php, 2010 (PS3)) followed by further source-mechanism studies [*Delouis et al.*, 2010; *Lay et al.*, 2010; *Koper et al.*, 2012; *Okal et al.*, 2012].

[3] Moreover, a network of superconducting gravimeters publishes data within the framework of the Global Geodynamic Project (GGP) (http://www.eas.slu.edu/GGP/ggphome.html). These earthquakes (together with the 2004 Sumatra earthquake) are thus the best instrumentally recorded giant events in the history of seismology. We have used gravity data from superconducting gravimeters to obtain radial mode amplitudes and to demonstrate how they constrain the M_{rr} components of the moment tensor and centroid depths of the Maule and Tohoku earthquakes.

2. Method

[4] The acceleration of a spherically symmetric, non-rotating, anelastic Earth at a receiver located at $\mathbf{x_r}(r_r, \vartheta_r, \varphi_r)$, that is excited by a moment-tensor source $\mathbf{M}$ situated at $\mathbf{x_s}(r_s, \vartheta_s, \varphi_s)$, is given by a superposition of spheroidal and toroidal modes,

$$\mathbf{a}(\mathbf{x_r}, \mathbf{x_s}, t) = \sum_k \mathbf{A}_k(\mathbf{x_r}, \mathbf{x_s}) \cos(\omega_k t) \exp\left(-\frac{\omega_k t}{2Q_k}\right). \quad (1)$$

The coefficients $\mathbf{A}_k(\mathbf{x_r}, \mathbf{x_s})$ are linearly proportional to the moment-tensor components, and they depend on a source-receiver geometry and the mode eigenfunctions; ω_k are angular frequencies and Q_k quality factors of the modes.

[5] If we consider a part of the response caused by a radial (degree-zero) mode, we can directly determine the coefficients $\mathbf{A}_k(\mathbf{x_r}, \mathbf{x_s})$ that are independent of the horizontal coordinates [*Dahlen and Tromp*, 1998, section 10.3],

$$\mathbf{A}_0(r_r, r_s) = \frac{U_r}{4\pi}\left[M_{rr}U_s' + \left(M_{\theta\theta} + M_{\phi\phi}\right)\frac{U_s}{r_s}\right]\mathbf{e_r}, \quad (2)$$

where the eigenfunction U and its derivative U' are only radially dependent, $U_r = U(r_r)$, $U_s = U(r_s)$, and M_{rr}, $M_{\theta\theta}$ and $M_{\phi\phi}$ are diagonal spherical polar components of the centroid moment tensor $\mathbf{M}$.

[6] If we take into account that the isotropic component of the source is negligible [*Kikuchi and Kanamori*, 1994; *Okal*, 1996], i.e., $M_{rr} = -(M_{\theta\theta} + M_{\phi\phi})$, the surface acceleration of a device caused by the radial modes depends on only the one component of the moment tensor M_{rr} and on the depth of the centroid,

$$\mathbf{A}_0(a, r_s) = \frac{U_a}{4\pi}\left(1 + \frac{2g}{\omega^2 a}\right)M_{rr}\left(U_s' - \frac{U_s}{r_s}\right)\mathbf{e_r}, \quad (3)$$

[1]Department of Geophysics, Faculty of Mathematics and Physics, Charles University in Prague, Prague, Czech Republic.
[2]Research Institute of Geodesy, Topography and Cartography, Zdiby, Czech Republic.

Corresponding author: E. Zábranová, Department of Geophysics, Faculty of Mathematics and Physics, Charles University in Prague, V Holešovičkách 2, CZ-18000, Prague, Czech Republic.

0094-8276/12/2012GL052850

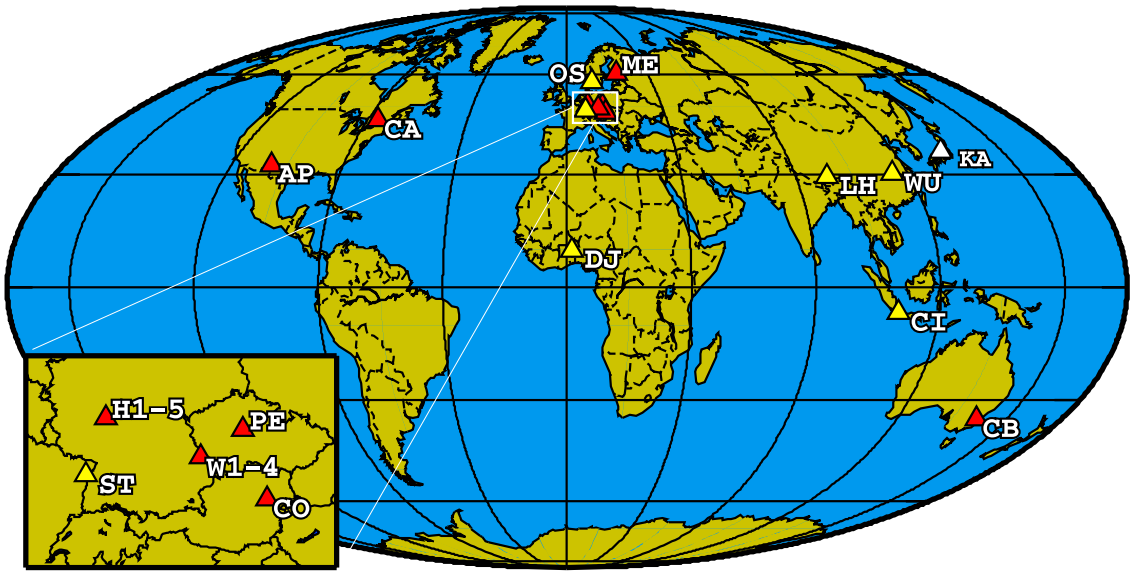

Figure 1. The triangles represent the SG sites used in this study. Red ones were employed for both events, white only for the 2010 Maule earthquake and yellow only for the 2011 Tohoku earthquake.

where $U_a = U(a)$ and the free-air change in gravity due to the radial displacement of the device is included [e.g., *Dahlen and Tromp*, 1998]. Therefore, simultaneous employment of several radial modes enables, in principle, one to determine not only the M_{rr} component of the moment tensor but also the centroid depth [*Lundgren and Okal*, 1988]. The centroid represents a point source in space and time but megathrust events are represented by finite-source solutions in many applications where, e.g., dimension and/or directivity of the source play a role. We calculated spheroidal modes up to 1.7 mHz also for the finite-source solution by *Hayes et al.* [2011] and found that there are no significant effects if this finite source is replaced by a suitable point source [see also *Zábranová et al.*, 2012], where finite-source representations of the Tohoku event are taken into account. On the other hand, the calculated modal amplitudes—and, subsequently, the constraints on the moment tensor—depend on local values of elastic coefficients at the source, that is the clear shortcoming of a point-source representation.

[7] We calculate the eigenfrequencies and the eigenfunctions of the spherical equivalent-rock PREM [*Dziewonski and Anderson*, 1981], where the upper 3-km layer of water is replaced by a 1.2-km-thick rock-layer with the same mass, by means of our pseudospectral finite-difference matrix-eigenvalue approach [*Zábranová et al.*, 2009]. The frequencies and eigenfunctions of the degenerate multiplets evaluated by our code for the PREM were tested by the Mineos software package.

[8] If non-spherical corrections due to the rotation and ellipticity are considered in this degree-zero case, only the frequencies of modes are slightly shifted, so formulas (1)–(3) can again be used because each radial mode consists just of one singlet [*Dahlen and Tromp*, 1998], and coupling with other modes is negligible [*Davis et al.*, 2005]. Moreover, *Rosat et al.* [2007] showed that for a three-dimensional rotating elliptic Earth model, the difference between theoretically predicted minimum and maximum amplitudes of the ${}_0S_0$ mode reaches only 2%; therefore, we assume that excitation is almost independent of source-station horizontal geometry, and we averaged observed signals from different stations to suppress the noise.

3. Data Analysis and Results

[9] The data for the Maule (32 days) and Tohoku (20 days) earthquakes are freely available on the GGP web pages. Only the stations shown in Figure 1 were employed because the time series available from other stations were either too short or affected by gaps and/or steps. A high-pass Butterworth

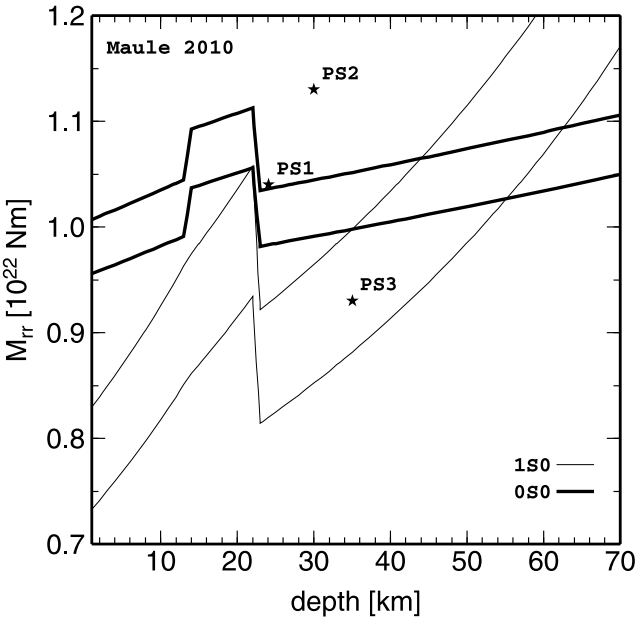

Figure 2. Dependence of the M_{rr} component of the centroid moment tensor on the centroid depth from the ${}_0S_0$ and ${}_1S_0$ amplitudes for the 2010 Maule earthquake. For each mode, the interval corresponding to ± one standard deviation of amplitude-spectra and quality factors is drawn. Stars denote published point-source solutions (PS1, PS2 and PS3).

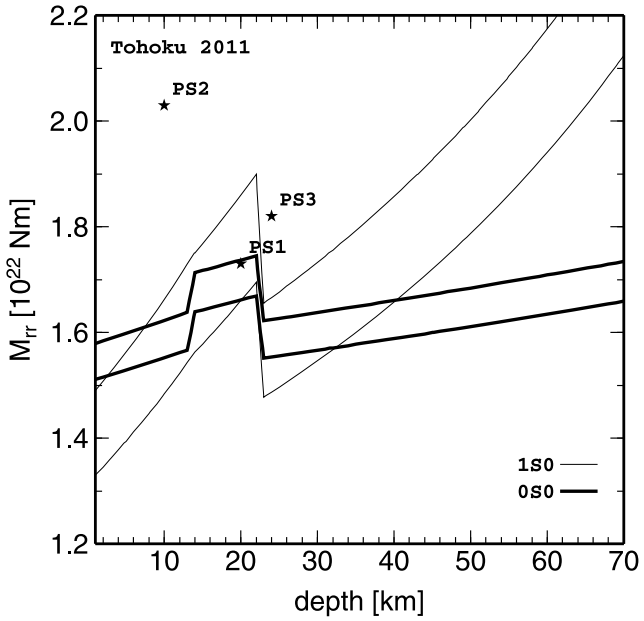

Figure 3. Dependence of the M_{rr} component of the centroid moment tensor on the centroid depth from the ${}_0S_0$ and ${}_1S_0$ amplitudes for the 2011 Tohoku earthquake. For each mode, the interval corresponding to ± one standard deviation of amplitude-spectra and quality factors is drawn. Stars denote published point-source solutions (PS1, PS2 and PS3).

filter (above 0.1 mHz) was used to remove local tides from raw gravity data (sampled at 1 s) corrected for atmospheric effects using locally recorded atmospheric pressure data and a nominal admittance factor of −3 nm/s^2/hPa.

[10] Figures 2 and 3 demonstrate the constraints on the M_{rr} component of the moment tensor and the depth of the Maule

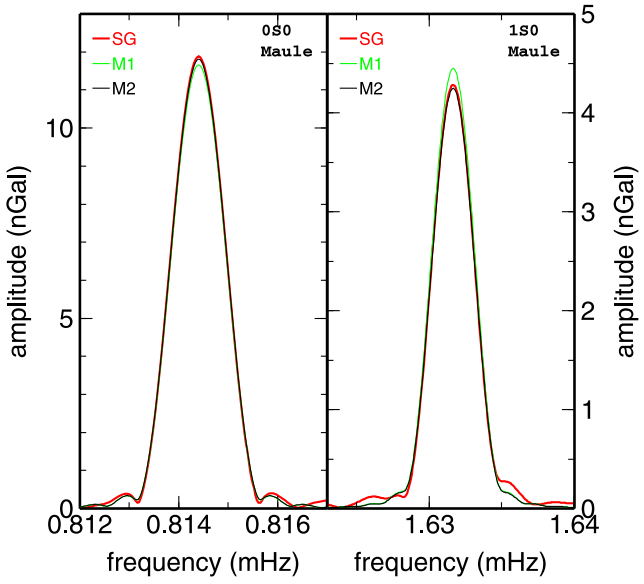

Figure 4. Vertical acceleration amplitude spectra of the modes ${}_0S_0$ and ${}_1S_0$ from the averaged SG data (red) and the two synthetics: M1 (green, depth 21 km; $M_{rr} = 1.055 \times 10^{22}$ Nm) and M2 (black, depth 44 km; $M_{rr} = 1.025 \times 10^{22}$ Nm) for the 2010 Maule earthquake. A Hann filter and Fourier transform were applied to 450- (170-)hour time series.

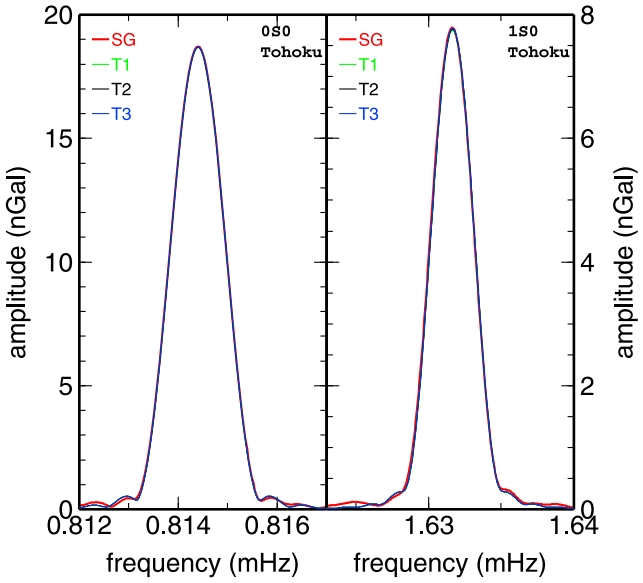

Figure 5. Vertical acceleration amplitude spectra of the modes ${}_0S_0$ and ${}_1S_0$ from the averaged SG data (red) and the three synthetics: T1 (green, depth 13 km; $M_{rr} = 1.60 \times 10^{22}$ Nm), T2 (black, depth 18 km; $M_{rr} = 1.69 \times 10^{22}$ Nm) and T3 (blue, depth 29 km; $M_{rr} = 1.60 \times 10^{22}$ Nm) for the 2011 Tohoku earthquake. A Hann filter and Fourier transform were applied to 450- (170-)hour time series.

M_w = 8.8 and Tohoku M_w = 9.1 earthquakes obtained from the amplitudes of ${}_0S_0$ and ${}_1S_0$. They are clearly isolated in the spectrum, and the level of observed noise is low (see the mode amplitudes in Figures 4 and 5). A Hann taper and Fourier transform were applied to averaged data signal and synthetic calculations. The synthetic solutions were found by a grid search in depth with 1-km step, using the fact that dependence of amplitude on the M_{rr} parameter is linear for a fixed depth.

[11] The quality factor Q is a key parameter, and its value used in synthetic calculations can substantially influence the results. For example, *Riedesel et al.* [1980] found that Q is between 5600 and 5833 for the ${}_0S_0$ mode and between 1850 and 1960 for the ${}_1S_0$ mode. Lower values for the ${}_0S_0$ mode were reported by *Roult et al.* [2006] (5489), *Xu et al.* [2008] (5400) and *Okal and Stein* [2009] (5579), who, on the other hand, obtained a higher value (2017) for the ${}_1S_0$ mode. We analyzed gravity data from the Maule and Tohoku earthquakes (32- and 20-days long records, respectively, for ${}_0S_0$, 13-days long records for ${}_1S_0$ and 5-days long records for ${}_2S_0$) using several shifted time windows and the fact that $Q^{-1} = T/(\pi\Delta t)\ln\frac{A_{ref}}{A}$ for each record, where T is period of a mode and Δt is time shift between time windows used to calculate spectral amplitudes A_{ref} and A. We found Q = 5500 ± 140 for the ${}_0S_0$ mode, Q = 2000 ± 80 for the ${}_1S_0$ mode and Q = 1120 ± 270 for the ${}_2S_0$ mode. ${}_2S_0$ would confine the depth even more than the ${}_1S_0$ mode if the Q factor were determined with a similar accuracy. However, the relative error is so high that we have not been able to use this mode as another meaningful constraint.

[12] In the case of Maule, we have employed three time series lasting up to 32 days for ${}_0S_0$ and three time series up to 8 days for ${}_1S_0$ to determine mode amplitudes as specified in

Table 1. The Lengths of Employed Time Windows and Corresponding Amplitude-Spectra Standard Deviations (Percent) for the Two Radial Modes

	${}_0S_0$			${}_1S_0$		
	760 h	450 h	350 h	190 h	170 h	150 h
Maule	1.5	1.7	1.7	3.3	3.5	3.7
Tohoku	x	1.3	1.5	3.0	2.9	2.9

Table 1. In the case of Tohoku, such long data sets are not available, and we were left with 20-day records. For each time window the standard deviation expressed in percents about averaged amplitude was calculated from the amplitudes obtained from individual station records.

[13] The depth-dependence of M_{rr} obtained from the ${}_0S_0$-mode-amplitude calculations is weak (jumps at depths of 13 and 22 km are caused by jumps in the radial derivatives of the mode displacement on the corresponding structural interfaces of the equivalent-rock PREM) and this mode thus confines the M_{rr} magnitudes into relatively narrow bands of $0.95–1.15 \times 10^{22}$ Nm for the Maule earthquake and $1.50–1.75 \times 10^{22}$ Nm for the Tohoku earthquake. On the other hand, the solution band produced by the ${}_1S_0$ mode is more depth-dependent, and it demonstrates that centroid depths should be located in the lower crust or just below the Moho for the Tohoku event but might be deeper for Maule.

[14] Figures 4 and 5 demonstrate an agreement in the amplitude spectra between the averaged SG data and the synthetics. We use 450-hour (${}_0S_0$) and 170-hour (${}_1S_0$) time series. Figure 4 shows two solutions (M1 and M2) at the depths 21 km ($M_{rr} = 1.055 \times 10^{22}$ Nm) and 44 km (1.025×10^{22} Nm) for the Maule earthquake. Figure 5 shows three solutions (T1, T2 and T3) at the depths 13 km (1.60×10^{22} Nm), 18 km (1.69×10^{22} Nm) and 29 km (1.60×10^{22} Nm) for the Tohoku earthquake.

4. Conclusions

[15] We have re-evaluated the quality factor Q of the ${}_0S_0$ mode ($Q = 5500 \pm 140$) and the ${}_1S_0$ mode ($Q = 2000 \pm 80$) and demonstrated that M_{rr} of the 2010 Maule and 2011 Tohoku earthquakes should fall within the intervals $0.95–1.15 \times 10^{22}$ Nm and $1.50–1.75 \times 10^{22}$ Nm, respectively, to yield the observed ${}_0S_0$-mode amplitude. Moreover, the ${}_1S_0$ mode provides constraints on the centroid depth. From the three rapid centroid solutions shown in Figures 2 and 3, only the PS1 M_{rr} component lies in the intervals mentioned above. The PS2 value is close to the upper limit for the Maule earthquake and clearly overestimates the Tohoku event. On the other hand, the PS3 value slightly underestimates the first event and overestimates the second earthquake. That these constraints on the M_{rr} component are not, in general, satisfactorily fulfilled, can be explained by the fact that radial modes are rather weak, as the non-diagonal moment-tensor terms dominate in the corresponding source solutions. Therefore, the weights of M_{rr} in full moment-tensor-waveform inversions are relatively small.

[16] **Acknowledgments.** We thank F. Gallovič for long and fruitful discussions, J. Zahradník for encouragement, J. Velímský for broad support, C. Bina for comments, and two anonymous reviewers for constructive reviews. This research was supported by the Grant Agency of the Charles University under projects 2010–141610 and 2012–265308 and by research project MSM 0021620860 of the Czech Ministry of Education, Youth and Sports.

[17] The Editor thanks two anonymous reviewers for their assistance in evaluating this paper.

References

Dahlen, F. A., and J. Tromp (1998), *Theoretical Global Seismology*, Princeton Univ. Press, Princeton, N. J.

Davis, P., M. Ishii, and G. Masters (2005), An assessment of the accuracy of GSN sensor response information, *Seismol. Res. Lett.*, *76*, 678–683.

Delouis, B., J.-M. Nocquet, and M. Vallée (2010), Slip distribution of the February 27, 2010 Mw = 8.8 Maule earthquake, central Chile, from static and high-rate GPS, InSAR, and broadband teleseismic data, *Geophys. Res. Lett.*, *37*, L17305, doi:10.1029/2010GL043899.

Duputel, Z., L. Rivera, H. Kanamori, G. P. Hayes, B. Hirshorn, and S. Weinstein (2011), Real-time W phase inversion during the 2011 off the Pacific coast of Tohoku earthquake, *Earth Planets Space*, *63*, 535–539.

Dziewonski, A. M., and D. L. Anderson (1981), Preliminary reference Earth model, *Phys. Earth Planet. Inter.*, *25*, 297–356.

Hayes, G. P., X. Li, C. Ji, and T. Maeda (2011), Rapid source characterization of the 2011 Mw 9.0 off the Pacific coast of Tohoku earthquake, *Earth Planets Space*, *63*, 529–534.

Honda, R., et al. (2011), A complex rupture image of the 2011 off the Pacific coast of Tohoku earthquake revealed by the MeSO-net, *Earth Planets Space*, *63*, 583–588.

Kikuchi, M., and H. Kanamori (1994), The mechanism of the deep Bolivia earthquake of June 9, 1994, *Geophys. Res. Lett.*, *21*, 2341–2344.

Koper, K. D., A. R. Hutko, T. Lay, C. J. Ammon, and H. Kanamori (2011), Frequency-dependent rupture process of the 2011 Mw 9.0 Tohoku earthquake: Comparison of short-period P wave backprojection images and broadband seismic rupture models, *Earth Planets Space*, *63*, 599–602.

Koper, K. D., A. R. Hutko, T. Lay, and O. Sufri (2012), Imaging short-period seismic radiation from the 27 February 2010 Chile (M_W 8.8) earthquake by back-projection of *P*, *PP*, and *PKIKP* waves, *J. Geophys. Res.*, *117*, B02308, doi:10.1029/2011JB008576.

Kurahashi, S., and K. Irikura (2011), Source model for generating strong ground motions during the 2011 off the Pacific coast of Tohoku earthquake, *Earth Planets Space*, *63*, 571–576.

Lay, T., C. J. Ammon, H. Kanamori, K. D. Koper, O. Sufri, and A. R. Hutko (2010), Teleseismic inversion for rupture process of the 27 February 2010 Chile (Mw 8.8) earthquake, *Geophys. Res. Lett.*, *37*, L13301, doi:10.1029/2010GL043379.

Lundgren, P. R., and E. A. Okal (1988), Slab decoupling in the Tonga arc: The June 22, 1977, earthquake, *J. Geophys. Res.*, *93*, 13,355–13,366.

Nettles, M., G. Ekström, and H. C. Koss (2011), Centroid-moment-tensor analysis of the 2011 off the Pacific coast of Tohoku earthquake and its larger foreshocks and aftershocks, *Earth Planets Space*, *63*, 519–523.

Okal, E. A. (1996), Radial modes from the great 1994 Bolivian earthquake: No evidence for an isotropic component to the source, *Geophys. Res. Lett.*, *23*, 431–434.

Okal, E. A., and S. Stein (2009), Observations of ultra-long period normal modes from the 2004 Sumatra-Andaman earthquake, *Phys. Earth Planet. Inter.*, *175*, 53–62.

Okal, E. A., S. Hongsresawat, and S. Stein (2012), Split-mode evidence for no ultraslow component to the source of the 2010 Maule, Chile, earthquake, *Bull. Seismol. Soc. Am.*, *102*, 391–397.

Polet, J., and H. K. Thio (2011), Centroid-moment-tensor analysis of the 2011 off the Pacific coast of Tohoku earthquake and its larger foreshocks and aftershocks, *Earth Planets Space*, *63*, 519–523.

Riedesel, M., D. Agnew, J. Berger, and E. Gilbert(1980), Stacking for the frequencies and Qs of ${}_0S_0$ and ${}_1S_0$, *Geophys. J. R. Astron. Soc.*, *62*, 457–471.

Rosat, S., S. Watada, and T. Sato (2007), Geographical variations of the 0S0 normal mode amplitude: Predictions and observations after the Sumatra-Andaman earthquake, *Earth Planets Space*, *59*, 307–311.

Roult, G., S. Rosat, and E. Clévédé (2006), New determinations of Q quality factors and eigenfrequencies for the whole set of singlets of the Earth's normal modes ${}_0S_0$, ${}_0S_2$, ${}_0S_3$ and ${}_2S_1$ using superconducting gravimeter data from the GGP network, *J. Geod.*, *41*, 345–357.

Shao, G., X. Li, C. Ji, and T. Maeda (2011), Focal mechanism and slip history of the 2011 Mw 9.1 off the Pacific coast of Tohoku earthquake, constrained with teleseismic body and surface waves, *Earth Planets Space*, *63*, 559–564.

Suzuki, W., S. Aoi, H. Sekiguchi, and T. Kunugi (2011), Rupture process of the 2011 Tohoku-Oki mega-thrust earthquake (M9.0) inverted from strong-motion data, *Geophys. Res. Lett.*, *38*, L00G16, doi:10.1029/2011GL049136.

Xu, Y., D. Crossley, and R. B. Herrmann (2008), Amplitude and Q of ${}_0S_0$ from the Sumatra earthquake as recorded on superconducting gravimeters and seismometers, *Seismol. Res. Lett.*, *79*, 797–805.

Yokota, Y., K. Koketsu, Y. Fujii, K. Satake, S. Sakai, M. Shinohara, and T. Kanazawa (2011), Joint inversion of strong motion, teleseismic, geodetic, and tsunami datasets for the rupture process of the 2011 Tohoku earthquake, *Geophys. Res. Lett.*, *38*, L00G21, doi:10.1029/2011GL050098.

Yoshida, Y., K. Miyakoshi, and K. Irikura (2011), Source process of the 2011 off the Pacific coast of Tohoku earthquake inferred from waveform inversion with long-period strong-motion records, *Earth Planets Space*, *63*, 577–582.

Zábranová, E., L. Hanyk, and C. Matyska (2009), Matrix pseudospectral method for elastic tides modeling, in *Mission and Passion: Science*, edited by P. Holota, pp. 243–260, Czech Natl. Comm. of Geod. and Geophys., Prague.

Zábranová, E., C. Matyska, and L. Hanyk (2012), Tests of the 2011 Tohoku earthquake source models using free-oscillation data from GOPE, *Stud. Geophys. Geod.*, *56*, 585–594, doi:10.1007/s11200-011-9033-5.

Zhang, H., Z. Ge, and L. Ding (2011), Three sub-events composing the 2011 off the Pacific coast of Tohoku earthquake (Mw 9.0) inferred from rupture imaging by back-projecting teleseismic P waves, *Earth Planets Space*, *63*, 595–598.